

Advancements in Point Cloud Data Augmentation for Deep Learning: A Survey

Qinfeng Zhu, Lei Fan¹, Ningxin Weng

Department of Civil Engineering, Xi'an Jiaotong-Liverpool University, Suzhou 215123, China

Abstract: Point cloud has a wide range of applications in areas such as autonomous driving, mapping, navigation, scene reconstruction, and medical imaging. Due to its great potentials in these applications, point cloud processing has gained great attention in the field of computer vision. Among various point cloud processing techniques, deep learning (DL) has become one of the mainstream and effective methods for tasks such as detection, segmentation and classification. To reduce overfitting during training DL models and improve model performance especially when the amount and/or diversity of training data are limited, augmentation is often crucial. Although various point cloud data augmentation methods have been widely used in different point cloud processing tasks, there are currently no published systematic surveys or reviews of these methods. Therefore, this article surveys and discusses these methods and categorizes them into a taxonomy framework. Through the comprehensive evaluation and comparison of the augmentation methods, this article identifies their potentials and limitations and suggests possible future research directions. This work helps researchers gain a holistic understanding of the current status of point cloud data augmentation and promotes its wider application and development.

Keywords: Point Cloud; Augmentation; Deep Learning; Detection; Segmentation; Classification

1 Introduction

A point cloud comprises a collection of three-dimensional (3D) points in space. Point cloud data are typically acquired through sensors such as depth cameras, Light Detection and Ranging (LiDAR), and millimeter-wave radar. Point clouds have important and valuable applications in various application fields such as autonomous driving, 3D reconstruction, medical imaging, virtual reality, and augmented reality. In recent years, with the significant reduction in the cost of various sensors, researchers have shown increasing interest in the practical value of point cloud data, resulting in an increasing number of publications related to point cloud processing and analysis.

In deep learning (DL), training data are crucial. Well-created datasets can greatly improve the robustness and generalization of trained networks. Data augmentation refers to performing a series of specific data operations to change or expand the original data, thereby increasing the quantity and diversity of the data for reducing overfitting during training. By this means, the robustness and generalization ability of a DL model can be optimized to a certain extent. In other words, the model can perform better when it encounters samples that may not be well represented in the original training data. Data augmentation is almost always desirable when training a network using DL. Comprehensive developments have taken place in image data augmentation and text data augmentation, as reported in surveys [1, 2].

In DL training using images, various image benchmarks have very large training samples. However, since generating diverse labeled point cloud data is usually more challenging, there are only few

¹ Corresponding author.

public benchmark point cloud data, and usually with limited class labels and data diversity. In this case, the augmentation of point cloud data is often more important.

In many recently published research papers on point cloud processing tasks, researchers have tried various methods of augmenting point cloud data. These methods vary widely, making it difficult for researchers to choose an appropriate method. Currently, no systematic surveys or reviews have been published on point cloud data augmentation. In this article, we conduct a comprehensive survey of augmentation methods for point cloud data. Based on our survey, we propose a taxonomy of these augmentation methods, as shown in Figure 1. According to their complexity, they are divided into two main categories: basic and advanced point cloud augmentation. The subcategories of augmentation methods in this taxonomy are presented in detail in Sections 2 and 3.

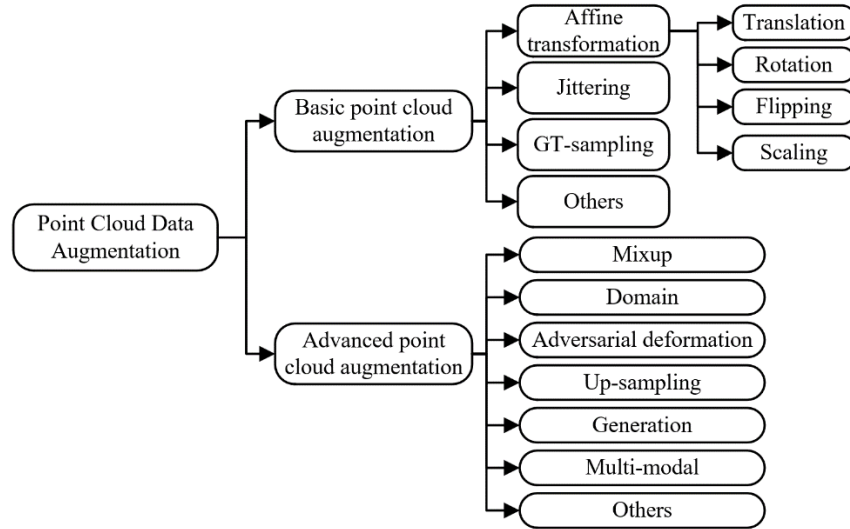


Figure 1: Taxonomy of point cloud data augmentation methods.

The main contributions of our article are as follows:

1. To the best of our knowledge, this is the *first* comprehensive survey of point cloud data augmentation methods. It covers recent advancements in point cloud data augmentation and provides suggestions for potential future work. According to the complexity and nature of augmentation operations, we propose a taxonomy of point cloud data augmentation methods.
2. This study summarizes and compares various point cloud data augmentation methods employed in representative studies on three typical point cloud processing tasks, namely detection, segmentation and classification.

The rest of this article is organized as follows. Section 2 introduces basic point cloud augmentation methods. Section 3 demonstrates advanced point cloud augmentation methods. In Section 4, we compare and discuss the reported performance of various combinations of augmentation methods and DL models on some common benchmark datasets for three tasks (i.e., detection, segmentation and classification). Finally, we conclude our survey and suggest potential future research directions.

2 Basic point cloud augmentation

When performing point cloud data augmentation, it is reasonable to first consider some basic operations, such as affine transformation, drop, jittering, and ground truth sampling (GT-sampling). Basic point cloud augmentation witnessed significant development in recent years, and some representative methods in this category are shown in Figure 2. In practical tasks, multiple basic operations are often combined to augment point cloud data.

In addition to aforementioned typical basic operations, there are a limited number of other basic operations (e.g., random noise point generation [3], dropping color [4]), which are simple but rarely used. These are not detailed in this article.

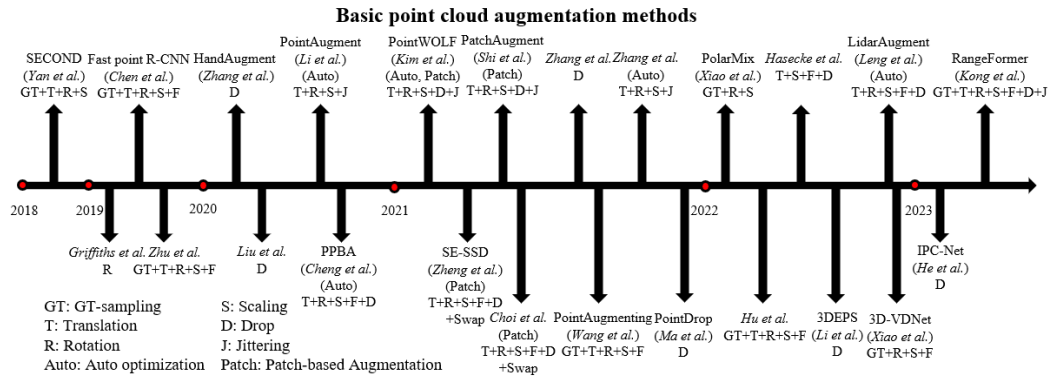


Figure 2: Chronological overview of representative basic point cloud augmentation methods.

2.1 Typical basic operations

2.1.1 Affine transformation

Affine transformation refers to a transformation of an affine space, which preserves collinearity and distance ratios. In the context of image data augmentation, commonly used affine transformation methods include scaling, translation, rotation, reflection and shear. Similarly, affine transformation can also be applied to point cloud data augmentation. Typical methods include *translation*, *rotation*, *flipping* and *scaling*, and have been widely used to generate additional new training data. All these operations can be applied to the entire set of point cloud data, or to a few selected *instances* in the point cloud data using specific strategies (an instance refers to a semantic object in point cloud data, such as the point cloud data representing a vehicle), or to specific part(s) of selected instances.

Translation represents the operation of translating selected point cloud data according to a specific distance and direction. This augmentation increases data diversity and also enables DL models to better learn instances at various locations, making the model less affected by instance positions. Translation is typically used in conjunction with other basic operations.

Rotation represents the operation of rotating selected point cloud data according to a specified direction and angle. This augmentation can be used to simulate different object poses or sensor viewpoints, thereby enhancing DL models to handle instances' pose variations. In point cloud processing tasks, rotation augmentation is sometimes used alone [5-10]. However, in most cases, it is used in conjunction with other basic operations.

Scaling represents the operation of performing a scale transformation on selected point cloud data. Scaling augmentation can simulate various object sizes, thereby increasing data diversity and enhancing the adaptability of DL models to scale variations. When scaling is used as an augmentation technique, it is commonly used along with other basic operations.

Flipping represents the operation of flipping selected point cloud data along a specified axis (usually the central y-axis or principal axis) to generate new training data. This method can simulate the orientation of instances, thereby enhancing the generalization ability of DL models to instance orientations and symmetry features, and also expanding the training data. Flipping is often used jointly with other basic operations.

These affine transformation operations are simple and effective, but they may face the challenges of introducing semantic inaccuracies. For example, translation may cause instances in the training data to exist in semantically inappropriate positions, while rotation may cause instances to have incorrect semantic orientations.

2.1.2 Drop

Drop refers to discarding some data points in point cloud data. The selection of points to remove is determined by specific strategies formulated by researchers. The discarded points can be all points representing some part(s) of the whole point cloud data, or are constituted by randomly selected points of instance(s) or a scene. This method, to some extent, can simulate the situation of missing data points such as occluded point cloud data, and enhance the generalization ability of DL models. However, losing excessive or key point cloud information by drop augmentation may affect the performance of DL models. This method can also defend against point cloud attacks to a certain extent [11].

Using the idea of 2D random cropping to select discarded points, Zhang et al. [11] generated a specific number and size of cuboids in the point cloud data, and randomly discarded points within a specific proportion of cuboids. This method can force a model to better learn local geometric features, because the model needs to predict the content of the discarded information through other available geometric features. However, this random dropping method may lead to loss of meaningful feature information. To simulate the data loss situation, IPC-Net [12] uses the idea of random erase. This method randomly selects a location in a point cloud instance in the 2D view as the centroid, and then discards all points inside a circle with the centroid as the center and a random length as the radius. However, these random drop algorithms do not consider the distinctions between points.

To honor key points or semantic information in point cloud data, more advanced drop algorithms have also been developed. PointDrop [13] uses an adversarial learning method to find key points in the point cloud data and drop them to obtain more challenging sparse samples for training. To better perform gesture recognition, HandAugment [14] first roughly extracts the point cloud data representing the hand and its surrounding parts, and then uses a neural network to find and discard useless data outside the spatial extent of the hand. Since most point cloud processing tasks do not require the removal of invalid regions, this method is difficult to extend to other tasks. 3DEPS [15], as shown in Figure 3, divides the edge part and non-edge part of the point cloud data representing plants and performs different degrees of dropping on them, which protects the structural semantic information of the point cloud data representing plants to a certain extent. However, if this method is extended to other types of objects (such as cars), whose edge features may not be as complex as plants, the drop strategy of 3DEPS may be less effective.

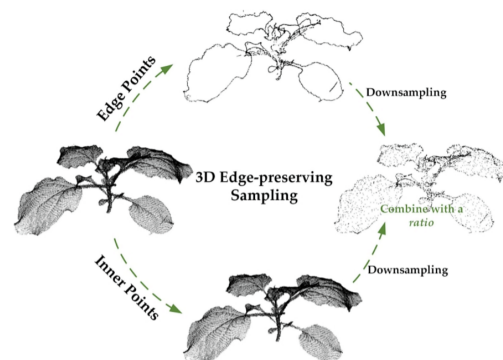


Figure 3: Example of augmentation using 3DEPS [15]

2.1.3 Jittering

Jittering refers to applying a certain degree of perturbation to points in a point cloud. First, the magnitude of perturbation is determined by users. Second, a perturbation vector is generated for each point according to the perturbation magnitude determined. This perturbation vector is usually generated using random sampling or random number methods. The last step is to perturb the points. In this step, each point in the point cloud is perturbed by its corresponding perturbation vector and transformed into a perturbed point.

Jittering can simulate the noise phenomenon of point cloud data in the real world and enhance a DL model's resistance to noise. At the same time, the method strengthens the edge information through small perturbations, and the model can better capture the local geometric structure. However, excessive perturbation may also destroy the structural features of the point cloud, thereby affecting the performance of the model.

2.1.4 GT-sampling

GT-sampling refers to adding labeled instances to a training set, where labeled ground-truth instances come from the same training set or other datasets. GT-sampling is one of the most commonly used methods for point cloud data augmentation due to its ease of use and effectiveness, and is usually used in combination with other basic operations (to each added instance). It was first proposed in SECOND [16], which randomly selects labeled instances in the dataset and adds them to the training set, and then removes those added instances that are collided with existing objects in the training set. Many subsequent GT-sampling methods [17-26] were formulated using the same or similar strategies as SECOND.

Although such GT-sampling strategies are effective, it still encounters some challenges. Added instances may encounter semantic problems. More specifically, added instances may be placed inappropriately and thus not fit the context of scene environment (e.g., an added car on tree, an added car colliding with pedestrian). Some researchers improved GT-sampling for more realistic semantics. Fast point R-CNN [27] copies the point cloud data of a small area around the instance that needs to be replicated in order to better preserve the contextual information of the added instances. Although this strategy preserves contextual information to a certain extent, it does not actually solve rationality, because instances may still not match the real environment. Its effectiveness in complex scenes needs to be further verified. To improve the semantic plausibility, Hu et al. [28] proposed CA-AUG, which calculates the reasonable locations where point cloud instances can be placed and adds labeled instances in these reasonable areas, as shown in Figure 4.

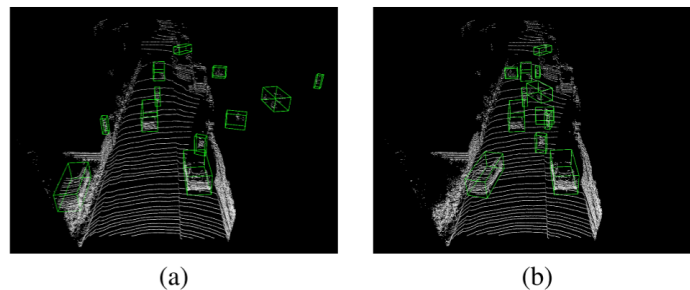


Figure 4: (a) normal GT-sampling, (b) CA-AUG, which improved the plausibility of the context semantics when adding instances [28]

Some researchers also tried to improve the GT-sampling strategy to deal with the class imbalance problem. RangeFormer [29] copies ground truth objects of the class with the least number of instances to other training scenes and changes their embedded global positions along the azimuth.

Zhu et al. [30] proposed dataset sampling (DS) and ground truth augmentation (GT-AUG) to deal with class imbalance in autonomous driving scenes. GT-AUG is an augmentation method similar to SECOND [16], using GT-sampling jointly with other basic operations. DS selects instances in the minority class and adds them to the training set to make the distribution of instances more balanced. But neither of these approaches considers the semantics of replicated instances in new scenes.

The aforementioned GT-sampling methods may destroy the structure of the point cloud data where instances are added. In other words, some data points may be occluded by added instance(s). PointAugmenting [31] considers point cloud data plausibility in cases where added instances using GT-sampling results in occlusion. This method not only avoids collisions between instances, but also filters out the occluded points and preserves the points close to the sensor according to the level of occlusion. Similarly, to keep GT-sampling semantically plausible without breaking LiDAR’s point cloud data structure, Hasecke et al. [32] designed a competition mechanism for point injection. When labeled instances of minority classes are added to point cloud data and occlusion happens, points closer to the sensor will be kept while points farther away will be deleted. It has the advantage that labeled instances can be inserted behind occluders (e.g. inserting a car instance behind a street lamp with reasonable semantics). Since translation can change point-to-sensor distance, it is not considered for protecting the sensor structure.

Xiao et al. [33] pointed out that the method proposed by Hasecke et al. [32] is still based on copy-paste mode, resulting in a vertical overlap between the inserted instance and the target scene. To avoid this problem, they proposed 3D-VDNet [33], which formulates a selection strategy for insertion locations based on vertical distribution characteristics (VDC) to avoid vertical overlap and select locations with surrounding environment information. However, this approach is not plug-and-play and cannot be extended to non-VDC-based models.

In BEV (bird's eye view), PolarMix [34] makes some special improvements to the GT-sampling strategy. This method swaps all points within the fan-shaped area of a specific azimuth angle in two scenes. The method then rotates several selected instances around a center point in the BEV and pastes them into other scenes to create new training samples.

2.2 Global and local point cloud augmentation

Point cloud data augmentation can be applied globally or locally. In global point cloud augmentation, the entire point cloud data are augmented simultaneously. For example, an affine transformation can be applied to transform all points in a specific scene to obtain an augmented point cloud, as shown in Figure 5. Local point cloud augmentation refers to the case where augmentation is performed only on specific part(s) or instance(s) in the whole point cloud data. For instance, an affine transformation can be applied to transform specific instance(s) in a scene while keeping the overall scene unchanged, as shown in Figure 6.

Patch-based augmentation is a special case of local augmentation, where specific part(s) of an instance in point cloud data are augmented. In this augmentation, local part(s) of instance(s) are selected using specific techniques and are subject to various point cloud transformation operations. This enables DL models to better learn the local features of point cloud instances, thereby improving the model performance in point cloud processing and analysis. It should be noted that in addition to typical basic operations, 'swap' operations [3, 35] are sometimes used for patch-based augmentation, where all the point cloud data of the two augmented parts are swapped. SE-SSD [35] partitions the cuboid of the car instance into six pyramids (one for each face), as shown in Figure 7. Point cloud data in these six pyramids are individually augmented using random discard, swap, and/or sparseness operations. This method can strengthen the model's perception of the car’s shape, but may not work for other types of objects. Likewise, PA-AUG proposed by Choi et al. [3] divides

a given instance into 4 or 8 cuboids and uses several augmentation operations on the point cloud data in these cuboids respectively. PA-AUG is not only applicable to the perception of cars, but also to the perception of other classes.

PointWOLF [36] performs smooth non-rigid deformations on parts of a given instance, as shown in Figure 8. It selects multiple anchor points through the method of farthest point sampling, and then deforms the local areas in the range of these anchor points, respectively. This approach generates visually realistic and diverse new training data, but may not be suitable for certain classes of regularly shaped objects, such as cars. PatchAugment [37] uses k nearest neighbor (k-NN) or sphere querying [38] to divide a given instance into many grouped points, and then performs a combination of basic operations on these groups together.

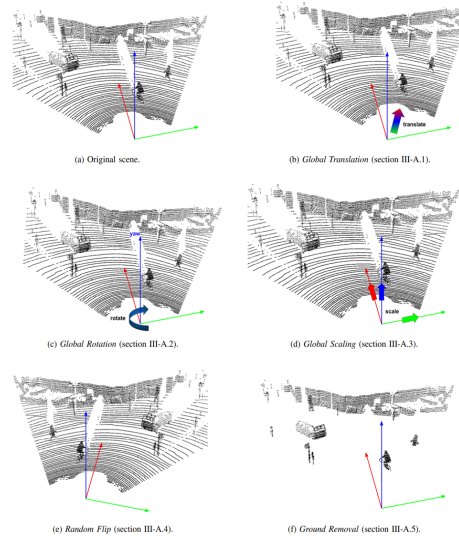


Figure 5: Visualization of global augmentation [39]

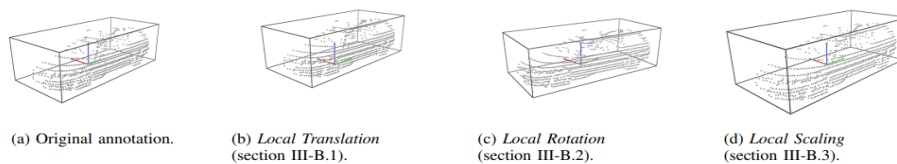


Figure 6: Visualization of local augmentation [39]

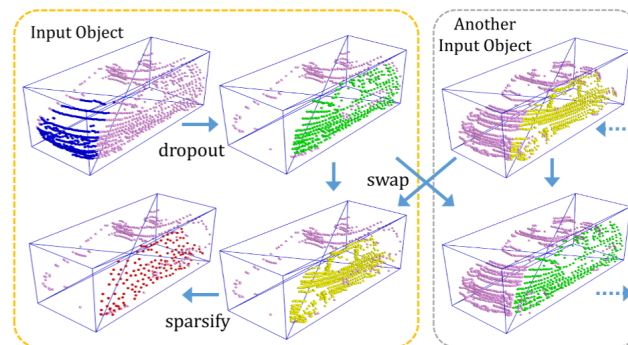


Figure 7: Example of augmentation using SE-SSD [35]

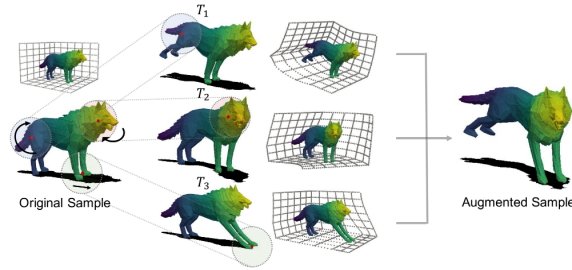


Figure 8: Example of augmentation using PointWOLF [36]

2.3 Combination of basic operations

When considering basic point cloud data augmentation, researchers usually use a combination of individual basic operations to augment point cloud data for better performance. For example, SECOND [16] uses a combination of GT-sampling, global rotation, global scaling, local rotation (to each ground truth instance), and local translation (to each ground truth instance). PatchAugment [37] applies random drop, random scaling, random rotation, random translation, and random jittering operations to parts of a given instance in point cloud data. Combinations of basic operations can be found in many other studies (e.g. [4, 17-24, 38, 40-72]). In these studies, researchers' choice of individual basic operations to combine is often based on extensive trial experiments or practical experience. Therefore, the combination used in each of those studies varies and is not detailed in this section. However, researchers also developed special methods to automatically obtain the optimal combination of basic operations and the associated parameters through the training of neural networks. These methods are defined as *Auto optimization* in this article.

PointAugment [73] is an end-to-end network capable of automatically selecting the best combination of augmentation operations from rotation, scaling, translation and jittering. Its network framework is shown in Figure 9. It uses an augmentor to augment the input samples to obtain augmented samples, and then trains both the input samples and the augmented samples in the classifier, and feeds back the result to the augmentor. Compared to PointAugment, Zhang et al. [74] proposed an automatic augmentation method named AdaPC, based on a two-layer optimization framework. Their method employs some basic operations (i.e., scaling, rotation, and translation) in the augmentor, and augments point cloud data with the minimized validation loss. This method was reported to be able to generalize to more challenging scenes. These two methods were designed to automatically select the optimal combination of basic operations for point cloud classification, but their applications to other tasks need further verifications.

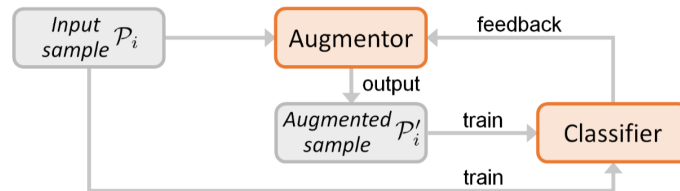


Figure 9: Overview of the PointAugment framework [73]

Progressive Population Based Augmentation (PPBA) [75] uses four basic operations in training. It uses two basic operations for data augmentation in each iteration, narrows the search space through continuous iterations, and finds the best parameters in iterations. This method can effectively improve the model performance in point cloud detection and is considered to have the potential to be extended to other point cloud processing tasks. PointWOLF [36] introduced in Section 2.2 is also an effective auto optimization augmentation tuning method (AugTune), which can adaptively

control the parameters of point cloud augmentation during training to generate targeted augmented data. AugTune is able to adaptively and effectively augment local regions of point cloud data.

The aforementioned auto optimization methods consider only a few basic operations. This is because if a model needs to find optimal parameters for many basic operations in auto optimization, the search space becomes very large. LidarAugment [76] uses factorization and alignment search space, significantly reduces hyperparameters and computational complexity, and automatically finds the optimal augmentation scheme among 10 augmentation operations.

Although auto optimization can adaptively select augmentation methods and parameters, such methods have the risk of overfitting. The reason for this is that a model may overfit to a particular pattern of variation in the training data and not fit well with other data.

3 Advanced point cloud augmentation

In addition to basic operations, many researchers have developed advanced augmentation methods for point cloud data, which apply more complex transformations or finer strategies to augment point cloud data for data diversity and authenticity. The development timeline of representative advanced augmentation methods is shown in Figure 10. It shows that many new advanced methods for point cloud data augmentation started to emerge after 2019. According to the nature of these advanced methods, they are further classified into mixup augmentation, domain augmentation, adversarial deformation augmentation, up-sampling augmentation, generation augmentation, multi-modal augmentation, and others.

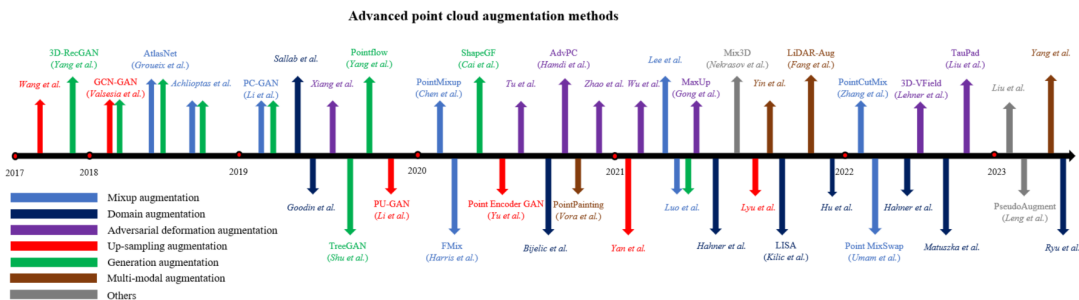


Figure 10: Chronological overview of representative advanced point cloud augmentation methods.

3.1 Mixup augmentation

Mixup [77] was first introduced in 2018, and has been widely used in the field of image classification. Its idea is to randomly select two images and mix them in a certain ratio to form a new image. Some researchers [78, 79] introduced this method into the point cloud classification task, in which two point cloud samples are randomly selected and mixed in a certain proportion to generate new point cloud samples to participate in training.

There are various techniques for mixing selected point cloud samples. For example, PointMixup [80] devises a linear interpolation method to generate mixed point clouds using an optimal distribution of path functions, which finds the shortest path between point clouds. Figure 11 shows some examples of mixed point cloud samples using PointMixup. However, this method may destroy the structural information of point cloud data [81]. To address this problem, Rigid Subset Mix (RSMix) proposed by Lee et al. [81] provides a neighboring function that can extract subsets and perform fusion while preserving the original shape in the point cloud.

PointCutMix [82] establishes the correspondence relationship of points based on the morphing and sampling network [83] between two point cloud samples and performs the mixup operation by exchanging these points. FMix [84] provides a novel mixup strategy that generates arbitrarily

shaped random masks between two point clouds and swaps the points in the masks between point clouds. Although the method works for one-, two- and three-dimensional cases, it performs poorly in ModelNet10 [85]. Point MixSwap [86] is the first method to introduce an attention mechanism into point cloud mixup. As an end-to-end method, it uses an attention module to decompose two point cloud samples into several disjoint regions, and completes mixup by exchanging points in these regions.

Some generative models have the ability to perform mixup operations, which are often referred to as 'interpolation' by their authors. These models map instances to their latent representations. In the latent space, the low-dimensional feature vectors of two samples are weighted and summed to map back to the data space to generate mixup samples. Achlioptas et al. [79] introduced a deep autoencoder (AE) network for point cloud generation. One of its uses is to perform mixup operations between point cloud data. PC-GAN [87] explores the possibility of introducing generative adversarial network (GAN) into point cloud generation, which uses a smaller network than that from Achlioptas et al. [79] and obtains better generation results. Inspired by non-equilibrium thermodynamic diffusion processes, Luo et al. [88] abstracted point cloud generation as a process of back diffusion of noise into a desired shape, thereby performing mixup between two point cloud samples in latent space.

Mixup methods effectively increase the diversity of training data by generating mixed point cloud samples. Moreover, models can learn intermediate states between labels, making them more robust during testing. However, mixup tends to significantly destroy semantic information, making it difficult to apply to scenarios other than classification.

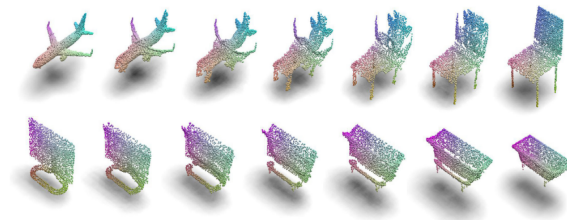


Figure 11: Examples of mixup between different classes at different degrees of mixup [80]

3.2 Domain augmentation

In DL-based point cloud processing tasks, training and testing data may originate from different data domains, such as different environments, location, time and/or sensors. Domain gap may exhibit different data characteristics, resulting in significant performance degradation of point cloud processing models [89]. That is to say, in different environments such as rainy or foggy weather, or when using different configurations or models of LiDAR sensors, the characteristics of obtained point cloud data vary, posing a big challenge to DL models. Domain augmentation is an augmentation approach that simulates training data from different domains to alleviate the problem of domain gap. This type of augmentation is often achieved by incorporating samples that mimic the characteristics of various domains into the training data.

A major challenge in point cloud processing comes from the influence of adverse weather conditions. Changes in the environmental domain, such as severe rainfall, can greatly affect the performance of point cloud processing models [90]. Bijelic et al. [91] collected point cloud data in severe weather along a distance of over 10,000 kilometers, but these data were difficult to use for training due to extreme weather. In order to improve the effect of bad weather on point cloud processing, researchers simulated point cloud data under harsh environment domains. Hahner et al. [92] used physical modeling to simulate different degrees of fog in their dataset to alleviate the

impact of fog on point cloud processing, and generated point cloud data under foggy weather as training data. Later, Hahner et al. [93] continued to use physical modeling to simulate a point cloud dataset under snowy weather, as shown in Figure 12. The method not only modifies beam measurements, but also simulates ground moisture for realism. Similar work was done by Kilic et al. [94], who simulated point cloud scenes of rain, snow and fog using physical modeling.

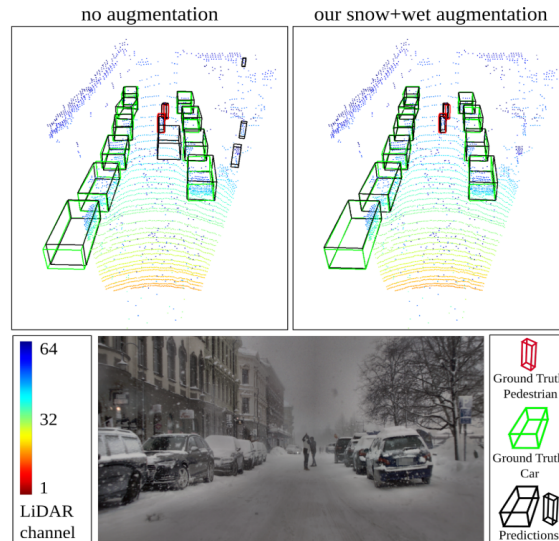


Figure 12: Example of environment domain augmentation: the point cloud data in the upper right corner simulate severe snowfall against the original point cloud data in the upper left corner. The plot at the bottom shows the RGB image as a reference. [93]

The characteristics of point cloud data vary depending on the configuration or model of sensors (e.g. number and angle of laser beam). Sensor domain augmentation can be used to simulate data domains of different sensors. Hu et al. [95] augmented point cloud data by simulating the point cloud characteristics of distant samples according to the characteristics of LiDAR sensors. The augmented point cloud data serve as new training data to improve the DL model's ability to detect instances far from the sensor. Matuszka et al. [96] introduced the two-dimensional zoom augmentation method [97] into 3D, and simulated the zooming of the LiDAR sensor according to the LiDAR intrinsics. While keeping the projection unchanged, the method uses virtual sensors to simulate the characteristics of point cloud instances at different distances to expand the training set, enabling the model to generalize to distant instances.

To simulate high-resolution point cloud data, Sallab et al. [98] simulated the sensor model based on CycleGAN [99] and simulated real and dense point cloud data. This method can also simulate synthetic data into real point cloud data according to the sensor model. According to the sensor characteristics, Ryu et al. [100] simulated the point cloud data obtained by other LiDAR configurations or models, so as to use them as training data to alleviate the sensor-bias problem.

3.3 Adversarial deformation augmentation

Adversarial deformation augmentation refers to using adversarial learning to perturb point cloud data to obtain augmented point cloud data. It employs an adversarial approach to deform training data to generate deformed point cloud data, which effectively enhances the diversity of training samples. This augmentation technique enhances the ability of DL models to generalize to out-of-domain samples.

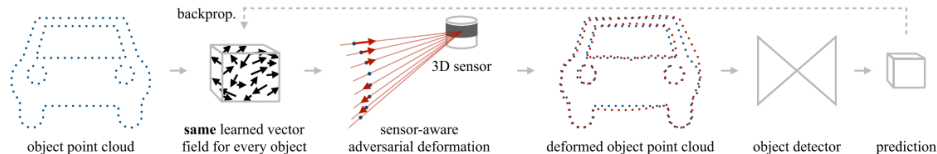


Figure 13: Example of adversarial deformation augmentation: 3D-VField deforms the point cloud data through adversarial learning [101]

3D-VField [101] uses adversarial learning to reasonably perturb the raw point cloud data, so that the points of an instance slide along the ray direction of the sensor view, to obtain augmented point cloud data, as shown in Figure 13. MaxUp [102] uses lightweight adversarial learning to generate and enforce a set of random perturbations on point cloud data and minimize the worst-case loss in the augmented point cloud data. Tu et al. [103] used an adversarial approach to add random meshes on top of the car in order to improve the model robustness in cases where objects are mounted on top of cars.

Only a few researchers have tried to augment point cloud data using adversarial attacks. For example, Wu et al. [104] used adversarial samples as augmented data for training to make the point cloud completion model more robust. Liu et al. [105] proposed TauPad (a point cloud data augmentation tool) which uses adversarial attacks to guide data deformation to achieve data augmentation, however its effectiveness in various point cloud processing tasks has not been verified.

Most adversarial attack techniques are not originally designed for data augmentation. For example, Xiang et al. [106] introduced adversarial attacks into point cloud analysis, and they used adversarial point perturbation and adversarial point generation to attack point cloud models. However, the transferability of their method between different networks is not strong. To address this problem, AdvPC [107] performs transferable adversarial perturbations on point clouds, and has a high attack success rate on unseen networks. Zhao et al. [108] discovered the vulnerability of 3D models in isometry transformations, and proposed a white-box attack method and a black-box attack method, both of which have good transferability. Although the authors of these methods did not mention that their methods could be used for point cloud data augmentation, they only need to add the generated adversarial samples as augmented point cloud data to the training set to become a data augmentation method. Doing this enables the model to learn the characteristics of adversarial samples during training, thereby enhancing the generalization ability of the model.

3.4 Up-sampling augmentation

Due to limitations such as occlusions, measurement angles and equipment, LiDAR sensors are not always able to obtain dense, high-quality point clouds during data acquisition. Therefore, the acquired point cloud data may be sparse and/or incomplete. Up-sampling methods, which algorithmically generate high-resolution (dense) point cloud data from the original low-resolution (sparse) point clouds, have attracted researchers' interest in recent years.

Although point cloud inpainting has not been explicitly designated as an augmentation method by researchers, it can be a good way to augment point cloud data. This method involves two steps: first choosing a down-sampling algorithm to down-sample the point cloud data in the training set, and second applying an inpainting method to the down-sampled data to obtain augmented data. It should be noted that down-sampling (i.e. the first step) is not always necessary, especially when the initial data are sparse. To take semantic rationality into account, Wang et al. [109] integrated GAN and Recurrent Convolutional Networks (RCN). Their method can achieve high-resolution inpainting results while considering context structure and semantic rationality, as shown in Figure

14. Since graph convolution can well extract local features of point cloud data, Valsesia et al. [110] successfully introduced graph convolution into GAN for inpainting tasks. However, the computational complexity of their method is relatively high. PU-GAN [111] is based on GAN, trains a generator network to generate densely distributed point sets, and uses a discriminator to evaluate and normalize the predictions, penalizing deviations from the expected generated results. However, this method has limited ability to fill large gaps in point cloud data.

Point cloud completion is a special form of point cloud up-sampling, which refers to predicting missing parts of point cloud data to generate a complete point cloud. Although the authors of point cloud completion did not state that it could be used for point cloud data augmentation, it can be improved into a point cloud data augmentation method. The steps are as follows. The first step is to deduct part(s) of point cloud data in the training set to become incomplete data, in which the strategy should be specifically designed according to actual requirements. The second step is to use the point cloud completion algorithm to generate the complete data as augmented data. It is important to note that it is not always necessary to carry out deduction (i.e. the first step), especially when the initial data are incomplete.

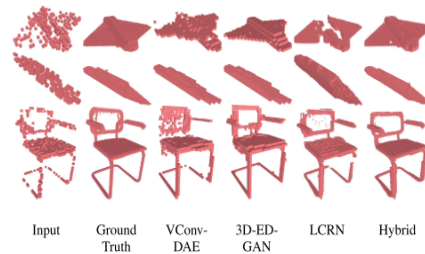


Figure 14: Examples of 3D inpainting with 50% injected noise on ShapeNet [112] test dataset [109]

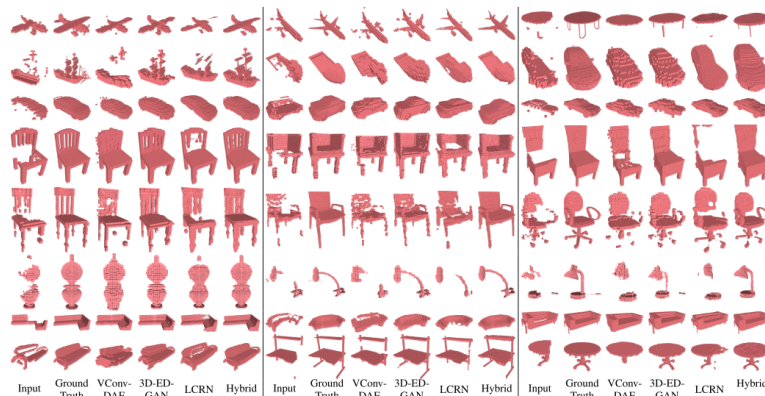


Figure 15: Examples of shape completion on ShapeNet [112]: testing points with simulated 3D scanner noise [109]

The method proposed by Wang et al. [109] can be used for point cloud completion, as shown in Figure 15. However, their method is based on voxelization, which may lose part of the information [113]. To directly process point cloud data, Yu et al. [113] proposed an end-to-end network based on point encoder GAN, which has strong generalization ability and prevents additional information loss. Yan et al. [114] completed the point cloud scene through the auxiliary information of adjacent frames to enhance the effect of point cloud segmentation. However, since information on adjacent frames may not be available, their method is not practical for segmenting point cloud data acquired in many real-world scenarios. To perform point cloud completion efficiently and meticulously, Lyu et al. [115] proposed the point diffusion-refinement paradigm, which generates uniform point cloud

data by denoising the diffusion probabilistic model and optimizes the rough parts in the generated point cloud.

The aforementioned techniques of inpainting and completion essentially perform data up-sampling, although the original point cloud data may initially be down-sampled when needed. As discussed, this approach has not been explored by researchers as an augmentation approach, but is deemed to be an innovative means of augmenting point cloud data.

3.5 Generation augmentation

Point cloud generation refers to the use of generative models to train datasets and generate new point cloud instances to simulate or represent the point cloud data characteristics of instances in the real world. With the advancement of generation models such as GAN and diffusion models, it has widely been used in various fields. Although point cloud generation has not been specifically explored as a point cloud data augmentation method in related studies, we believe it is a direct and useful means of point cloud data augmentation. This method is referred to as generation augmentation.

Generative models can generate diverse synthetic point cloud samples with varying structure, shape, local details, etc. These synthetic samples can be used for point cloud data augmentation. The method proposed by Valsesia et al. [110], mentioned in Section 3.4 (up-sampling augmentation), can also diversely generate point cloud data. Based on the tree-structured graph convolution network, TreeGAN [116] is a GAN that can generate point cloud data in an unsupervised mode. Its network can better represent features through the ancestor information in the network, but has high computational complexity. Generative models [87, 88] used for mixup augmentation can also be used for generation augmentation. Figure 16(a) shows examples of generated synthetic point clouds instances.

Point cloud reconstruction is a special form of point cloud generation. In point cloud reconstruction, for a partially damaged or sparse point cloud instance, a trained generative model is used to reconstruct the point cloud instance to obtain dense and accurate point cloud instance that can represent the corresponding object in real world as accurately as possible. The point cloud generated by this means can be used as augmented data. Figure 16(b) shows examples of reconstructed point clouds. 3D-RecGAN [117] is an end-to-end point cloud reconstruction network that combines autoencoders and GAN to predict 3D structures in voxel space. It can reconstruct a fine and complete 3D structure from a voxel grid at any viewing angle. Generative model [78, 79] used for mixup augmentation can also be used for point cloud reconstruction.

Some generative models are capable of generating both synthetic point cloud samples and reconstructed point cloud samples. The point cloud generation model proposed by Luo et al. [88], mentioned in Section 3.1 (mixup augmentation), can generate synthetic point cloud data through a diffusion model, as shown in Figure 16(a). It can also be used in point cloud reconstruction, as shown in Figure 16(b). There is usually high complexity when training GAN [118]. To avoid this problem, Pointflow [118] uses a principled probabilistic framework. This method first learns the distribution of point cloud shapes and then learns the distribution of points in the shapes, so as to generate synthetic point cloud data or reconstruct point cloud data. ShapeGF [119] uses a score-based generative model that moves randomly generated sampling points to high-density regions predicted by the model, and can be used for both point cloud reconstruction and synthetic point cloud data generation.

Currently, in the field of point cloud generation, researchers have focused primarily on the quality of generated point cloud data based on some evaluation metrics [79, 118], rather than recognizing its potential for data augmentation. However, it is worth noting that point cloud generation methods can effectively expand the diversity of training samples by generating point cloud instances.

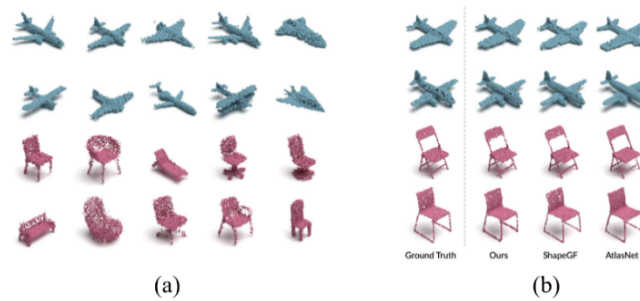


Figure 16: (a) Examples of generated synthetic point clouds instances [88], (b) Examples of reconstructed point cloud instances from different auto-encoders [88]

3.6 Multi-modal augmentation

Multi-modal augmentation represents the method of enhancing point cloud data with data of other modalities. Since images can provide complementary features of point cloud data, many researchers choose to introduce image modality to augment point cloud data. Compared with the point cloud modality, the image modality possesses rich semantic information and can be used to augment the point cloud modality by various means. For example, PointPainting [120] uses an image segmentation network in the image modality, and then projects the predicted segmentation categories and their scores onto the corresponding point cloud data for augmentation, as shown in Figure 17. Yin et al. [121] used an image detection algorithm in the image modality and then used the detection results to generate dense point cloud data to augment the original sparse point cloud data.

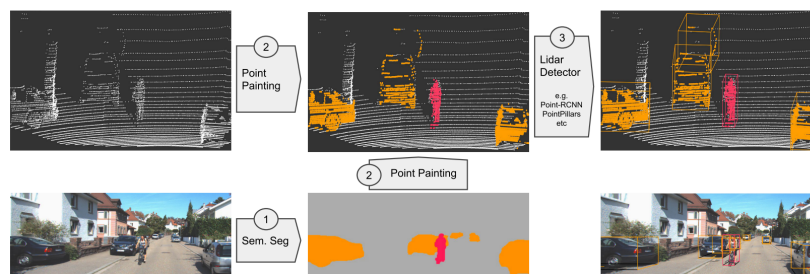


Figure 17: Multi-modal augmentation by PointPainting where the image modality was used to augment the point cloud data [120]

Other data modalities were also explored to augment point cloud data. For example, LiDAR-Aug [122] renders CAD models into point cloud data and selects random locations to place into the scene. Yang et al. [123] used synthetic datasets to enhance real datasets. They used the geometric partition method to cluster the synthetic point cloud and the real point cloud into a point set named superpoints, and then mixed the superpoints of the synthetic and the real point cloud in a certain proportion as a new training set.

However, multi-modal augmentation has its limitations. In many practical scenarios, acquiring data in the other modality may not be feasible, and meanwhile aligning the other modality with the point cloud modality poses challenges. Furthermore, point cloud augmentation using other modalities may not outperform algorithms specifically designed for multi-modal analysis.

3.7 Others

There are also special augmentation methods for point cloud data, which may not fall into any of the preceding categories due to their uniqueness. For example, Mix3D [124] blends two scenes to

create a new training sample, and this unique fusion approach produces promising augmentation results.

In semi-supervised learning, a teacher-student framework is often used. It is effective to use weak augmentation for the teacher network and strong data augmentation for the student network [69, 125]. Therefore, Liu et al. [125] designed an effective augmentation method in the student network. This method uses several horizontal and vertical lines to divide the point cloud area into rectangles of the same shape, shuffle these rectangles, and unshuffle them in the feature layer. In this way, the student network can focus on weak features, thereby enhancing the feature representation ability. However, this augmentation method may segment complete instances when shuffling, resulting in localization bias.

In semi-supervised learning, labeled data are used to train a simple model that predicts pseudo-labels for unlabeled samples. PseudoAugment [126] uses unlabeled data to augment the training data. This method removes the low-confidence point in the pseudo-labeled point cloud data generated by semi-supervised learning, then pastes the pseudo-object into the scene, and finally exchanges the pseudo-labeled scene with the labeled scene.

4 Application scenarios and performance

4.1 Application scenarios

Table 1 summarizes the application scenarios of some representative methods introduced in Section 2 and 3. According to the information reported by the authors of those methods, some methods in Table 1 are only used for a specific task, while the other methods can be used in multiple tasks.

Some methods (e.g. [106-108]) in adversarial deformation augmentation and all methods in up-sampling and generation augmentation are not shown in Table 1. The authors of these methods did not specify whether their methods could be used for data augmentation. However, as discussed in Section 3, these methods are considered as potential methods for point cloud data augmentation, and are expected to be applicable to various point cloud processing tasks.

Table 1. Implemented tasks of the point cloud augmentation methods considered, as reported by the authors of each method

Types of methods		Detection	Segmentation	Classification
Basic		[3, 11, 13, 16, 18-28, 30, 31, 33-35, 40, 42, 43, 49, 50, 53, 56, 60, 65, 67, 69, 75, 76]	[4, 10, 11, 15, 17, 29, 32, 34, 36, 38, 42, 44-46, 48, 51, 52, 54, 56, 58, 61, 62, 64, 66, 68, 70, 72]	[10-12, 36-38, 42, 44, 46, 48, 51, 56, 63, 64, 66, 73, 74]
Advanced	Mixup	-	-	[78-82, 84, 86-88]
	Domain	[92-96, 98]	[100]	-
	Adversarial Deformation	[101, 103]	-	[102]
	Multi-modal	[120, 121]	-	-
	Others	[122, 125, 126]	[123, 124]	-

4.2 Reported performance

Based on the information provided in the literature, it remains challenging to make a fair quantitative evaluation of the performance of point cloud data augmentation methods. In existing studies, testing usually involved various augmentation algorithms and multiple DL networks, and the combination (i.e. augmentation algorithm and DL network) yielding the highest score was selected to form their proposed method for specific point cloud processing task(s). Furthermore, the benchmark datasets used for testing (typically specific to point cloud processing tasks) are not always consistent. Therefore, the main purpose of Section 4.2 is to present point cloud data augmentation methods employed by the best-performing combination of augmentation and DL network in representative studies. It can also suggest the popularity of augmentation methods.

Some augmentation methods presented in Sections 2 and 3 are not considered for comparison. The environment domain augmentation algorithms in Section 3.2 are dedicated to the effects of severe weather using specific point cloud datasets, and as such they are not suitable for fair comparisons with other methods. Some methods have not been tested for point cloud data augmentation, and their performance data are unavailable. These methods include some algorithms [106-108] in adversarial deformation augmentation, and all methods in up-sampling and generation augmentation. As augmentation methods in semi-supervised learning usually train with partially labeled data, and some methods use relatively unpopular datasets, these methods are also excluded.

All compared methods are shown in Tables 2-7. Some authors integrated an augmentation method into their own point cloud processing algorithm, while others proposed a plug-and-play augmentation method to be used with an attractive baseline algorithm. For the latter, the corresponding baseline network is also shown in Tables 2-7.

4.2.1 Detection

KITTI [127] is a dataset for evaluating computer vision algorithms in autonomous driving scenarios. It is also one of the most commonly used datasets for 3D detection. There are also other large datasets such as nuScence [128] and Waymo [129] for algorithm evaluation. Table 2, 3, 4 show the performances of different algorithms on the KITTI dataset [127]. Table 5 shows the performance of different algorithms on the nuScence [128] and Waymo [129] datasets.

Basic augmentation methods can lead to better overall performance in detection tasks than advanced augmentation methods. As a simple and effective method, the combination of GT-sampling and other basic operations has been widely used in detection tasks. As an advanced method, multi-modal augmentation shows great potential in detection tasks. PointPainting [120] achieved the best overall performance in KITTI BEV test benchmark, and its detection of the Cyclists class is superior to other methods. The method proposed by Yin et al. [121] also performs well in nuScence [128], and its performance is very close to the best-performing network PointAugmenting [31] on nuScence.

Table 2. Comparative results of representative methods for the detection task on the KITTI 3D test benchmark. Notes (*applicable to Tables 2, 3 and 4*): 'E', 'M', and 'H' represent the easy, moderate, and hard categories of objects in this benchmark dataset, respectively. The Intersection over Union (IoU) threshold for 3D bounding boxes is 0.7 for Cars and 0.5 for Pedestrians and Cyclists. The '%' after the value is omitted. '-' means that the result is not available. The values in italics come from replicated tests by others. 'GT', 'T', 'R', 'S', 'F', 'D', 'J' represent GT-sampling, Translation, Rotation, Scaling, Flipping, Drop, Jittering, respectively.

Method			Baseline	Speed (fps)	Cars			Pedestrians			Cyclists			3D mAP Moderate
					E	M	H	E	M	H	E	M	H	
Basic	SA-SSD [23]	GT+T+R+S+F	-	25.00	88.75	79.79	74.16	-	-	-	-	-	-	-
	PointRCNN [19]	GT+T+R+S+F	-	<i>10.00</i>	85.94	75.76	68.32	49.43	41.78	38.63	73.93	59.60	53.59	59.05
	SECOND [16]	GT+T+R+S	-	20.00	83.13	73.66	66.2	51.07	42.56	37.29	70.51	53.85	46.90	56.69
	PointPillars [18]	GT+T+R+S+F	-	62.00	79.05	74.99	68.3	52.08	43.53	41.49	75.78	59.07	52.92	59.20
	3D-VDNet [33]	GT+R+S+F	-	38.00	87.13	78.05	72.9	-	-	-	-	-	-	-
	STD [22]	GT+T+R+S+F	-	10.00	86.61	77.63	76.06	53.08	44.24	41.97	78.89	62.53	55.77	61.47
	PV-RCNN [20]	GT+R+S+F	-	<i>12.50</i>	90.25	81.43	76.82	-	-	-	78.60	63.71	57.65	-
	SE-SSD [35]	Patch-based (T+R+S+F+D+Swap)	-	32.00	91.49	82.54	77.15	-	-	-	-	-	-	-
	PPBA [75]	Auto optimization (T+R+S+F+D)	StarNet [43]	-	84.16	77.65	71.21	52.65	44.08	41.54	79.42	61.99	55.34	61.24
	Voxelnet [40]	T+R+S	-	-	77.47	65.11	57.73	39.48	33.69	31.51	61.22	48.36	44.37	49.05
	StarNet [43]	-	-	-	81.63	73.99	67.07	48.58	41.25	39.66	73.14	58.29	52.58	57.84
	Point-GNN [49]	T+R+F+J	-	-	88.33	79.47	72.29	51.92	43.77	40.14	78.60	63.48	57.08	62.24
	MMF [53]	T+S	-	12.50	86.81	76.75	79.10	-	-	-	-	-	-	-
Frustum ConvNet [60]	T+R+S+F	-	-	85.88	76.51	68.08	52.37	45.61	41.49	79.58	64.68	57.03	62.27	
Advanced	3D-VField [101]	Adversarial deformation	Part-A ² [130]	<i>11.15</i>	89.65	79.26	78.62	-	-	-	-	-	-	-

Table 3. Comparative results of representative methods for the detection task on the KITTI 3D validation benchmark.

Method			Baseline	Speed (fps)	Cars			Pedestrians			Cyclists			3D mAP Moderate
					E	M	H	E	M	H	E	M	H	
Basic	CA-aug [28]	GT+T+R+S+F	PV-RCNN [20]	-	92.25	84.93	82.64	66.00	59.77	55.41	92.58	74.19	69.76	72.96
	Reconfigurable Voxels [21]	GT+F	-	47.00	88.65	78.22	76.21	80.50	65.82	60.24	61.63	54.08	50.33	66.04
	PointRCNN [19]	GT+T+R+S+F	-	10.00	88.88	78.63	77.38	62.16	58.00	50.53	91.72	72.47	68.18	69.70
	PV-RCNN [20]	GT+R+S+F	-	12.50	91.80	84.50	82.42	64.77	57.20	52.43	91.20	72.20	68.62	71.30
	SECOND [16]	GT+T+R+S	-	20.00	90.77	81.95	78.91	56.88	52.96	48.22	82.40	64.09	59.69	66.33
	3D-VDNet [33]	GT+R+S+F	-	38.00	90.15	81.66	78.97	-	-	-	-	-	-	-
	STD [22]	GT+T+R+S+F	-	10.00	89.70	79.80	79.30	73.90	66.60	62.90	88.50	72.80	67.90	73.07
	PA-AUG [3]	Patch-based (T+R+S+F+D+Swap)	PV-RCNN [20]	-	89.38	80.90	78.95	67.57	60.61	56.58	86.56	72.21	68.01	71.24
	Voxelnet [40]	T+R+S	-	-	81.97	65.46	62.85	57.86	53.42	48.87	67.17	47.65	45.11	55.51
Advanced	Pattern-Aware GT [95]	Domain augmentation	PV-RCNN [20]	-	92.13	84.79	82.56	65.99	58.57	53.66	90.38	72.03	67.96	71.80
	LiDAR-Aug [122]	Multi-modal	PV-RCNN [20]	-	90.18	84.23	78.95	65.05	58.90	55.52	-	-	-	-

Table 4. Comparative results of representative methods for the detection task on the KITTI BEV test benchmark.

Method			Baseline	Speed (fps)	Cars			Pedestrians			Cyclists			BEV mAP Moderate
					E	M	H	E	M	H	E	M	H	
Basic	SA-SSD [23]	GT+T+R+S+F	-	25.00	95.03	91.03	85.96	-	-	-	-	-	-	-
	SECOND [16]	GT+T+R+S	-	20.00	88.07	79.37	77.95	55.10	46.27	44.76	73.67	56.04	48.78	60.56
	PointPillars [18]	GT+T+R+S+F	-	62.00	88.35	86.1	79.83	58.66	50.23	47.19	79.14	62.25	56.00	66.19
	STD [22]	GT+T+R+S+F	-	10.00	89.66	87.76	86.89	60.99	51.39	45.89	81.04	65.32	57.85	68.16
	PV-RCNN [20]	GT+R+S+F	-	12.50	94.98	90.65	86.14	-	-	-	82.49	68.89	62.41	-
	3D-VDNet [33]	GT+R+S+F	-	38.00	91.72	88.15	84.65	-	-	-	-	-	-	-
	SE-SSD [35]	Patch-based (T+R+S+F+D+Swap)	-	32.00	95.68	91.84	86.72	-	-	-	-	-	-	-
	Voxelnet [40]	T+R+S	-	-	89.35	79.26	77.39	46.13	40.74	38.11	66.70	54.76	50.55	58.25
	Point-GNN [49]	T+R+F+J	-	-	93.11	89.17	83.9	55.36	47.07	44.61	81.17	67.28	59.67	67.84
	PIXOR [50]	R+F	-	10.75	81.70	77.05	72.95	-	-	-	-	-	-	-
MMF [53]	T+S	-	12.50	89.49	87.47	79.10	-	-	-	-	-	-	-	
Advanced	PointPainting [120]	Multi-modal	PointRCNN [19]	-	92.45	88.11	83.36	58.70	49.93	46.29	83.91	71.54	62.97	69.86

4.2.2 Segmentation

Two representative benchmark datasets for segmentation tasks are SemanticKITTI [131] and ShapeNet [112]. SemanticKITTI [131] is a large-scale dataset for semantic segmentation in automotive LiDAR scenes. ShapeNet [112] is a shape repository for richly annotated 3D CAD model representations. The performances of relevant methods on these two benchmark datasets are shown in Table 6.

For segmentation, the combinations of simple GT-sampling and other basic operations can produce strong overall performance. Based on the powerful Transformer model [132], RangeFormer [29] performs best overall in SemanticKITTI [131], which augments point cloud data by replicating classes with a small number of instances and changing positional embeddings by sliding in azimuth. Also based on the Transformer model, Stratified Transformer [4] uses only a combination of rotation, scaling and jittering to achieve state-of-the-art results in ShapeNetPart [112]. Transformer-based models have strong performance in point cloud segmentation, and their combination with other augmentation methods may achieve even better results.

Table 5. Comparative results of representative methods for the detection task on the nuScenes and Waymo benchmarks. On the nuScenes benchmark, mean Average Precision (mAP) and nuScenes detection score (NDS) are used for evaluation metrics. On the Waymo validation benchmark, mAP and mean Average Precision weighted by Heading (mAPH) are used. The IoU threshold for 3D bounding boxes is 0.7 for Vehicle and 0.5 for Pedestrians and Cyclists. The '%' after the value is omitted. '-' means that the result is not available. The values in italics come from replicated tests by others. 'GT', 'T', 'R', 'S', 'F', 'D' represent GT-sampling, Translation, Rotation, Scaling, Flipping, Drop, respectively.

Method			Baseline	nuScenes				Waymo v1.2 Validation					
				Validation		Test		Vehicle		Pedestrian		Cyclist	
				mAP	NDS	mAP	NDS	L1 mAP\mAPH	L2 mAP\mAPH	L1 mAP\mAPH	L2 mAP\mAPH	L1 mAP\mAPH	L2 mAP\mAPH
Basic	PolarMix [34]	GT+R+S	CenterNet [133]	55.4	61.1	-	-	-	-	-	-	-	-
	MEGVII [30]	GT+T+R+S+F	-	52.8	63.3	-	-	-	-	-	-	-	-
	PointAugmenting [31]	GT+T+R+S+F	-	-	-	66.8	71.0	67.41/-	62.70/-	75.42/-	70.55/-	76.29 /-	74.41 /-
	Reconfigurable Voxels [21]	GT+F	-	-	-	48.5	59.0	-	-	-	-	-	-
	PointPillars [18]	GT+T+R+S+F	-	31.5	-	30.5	45.3	63.30/62.70	55.20/54.70	68.90/56.60	60.40/49.10	-	-
	Hu et al. [24]	GT+T+R+F	-	35.4	-	35.0	-	-	-	-	-	-	-
	SECOND [16]	GT+T+R+S	-	48.8	58.6	31.6	46.8	72.27/71.69	63.85/63.33	68.70/58.18	60.72/51.31	60.62/59.28	58.34/57.05
	PV-RCNN [20]	GT+R+S+F	-	46.7	53.4	-	-	77.51/76.89	68.98/68.41	75.01/65.65	66.04/57.61	67.81/66.35	65.39/63.98
	LidarAugment [76]	Auto optimization (T+R+S+F+D)	SWFormer _{3f} [134]	-	-	-	-	80.90/80.40	72.80/72.40	84.40/80.70	76.80/73.20	-	-
StarNet [43]	-	-	-	-	-	-	53.70/-	-	66.80/-	-	-	-	
3D Auto Labeling [52]	T+R+S+F	-	-	-	-	-	84.50 /-	-	82.88/-	-	-	-	
AFDetV2 [67]	T+R+S	-	-	-	62.4	68.5	-	77.64/77.14	-	80.19/74.62	-	73.72/72.24	
Advanced	PointPainting [120]	Multi-modal	PointRCNN [19]	-	-	46.4	58.1	-	-	-	-	-	-
	Yin et al. [121]	Multi-modal	-	-	-	66.4	70.5	-	-	-	-	-	-

Table 6. Comparative results of representative methods for the segmentation task on the ShapeNetPart and SemanticKITTI benchmark. Overall Accuracy (OA) and mIoU are used for evaluation metrics. The '%' after the value is omitted. '-' means that the result is not available. 'GT', 'T', 'R', 'S', 'F', 'D', 'J' represent GT-sampling, Translation, Rotation, Scaling, Flipping, Drop, Jittering, respectively.

Method			Baseline	ShapeNetPart (mIoU)		SemanticKITTI		
				Cat (mIoU)	Ins (mIoU)	Speed (fps)	Test (mIoU)	Validation (mIoU)
Basic	PolarNet [8]	R	-	-	-	16.20	54.3	-
	PolarMix [34]	GT+R+S	SPVCNN [135]	-	-	-	-	66.2
	RangeFormer [29]	GT+T+R+S+F+D+J	-	-	-	-	73.3	-
	Hasecke et al. [32]	GT+T+S+F+D	Cylinder3D [136]	-	-	-	65.4	67.9
	Panoptic-PolarNet [17]	GT+T+R	-	-	-	11.62	59.5	64.5
	PointWOLF [36]	Patch-based (T+R+S+D+J)	DGCNN [137]	-	85.2	-	-	-
	Stratified Transformer [4]	R+S+J	-	85.1	86.6	-	-	-
	RS-CNN [46]	T+S+D	-	84.0	86.2	-	-	-
	PointNet [48]	R+J	-	80.4	83.7	-	14.6	-
	PointNet++ [38]	T+R	-	81.9	85.1	-	20.1	-
	MPF [54]	T+R+S+F+D	-	-	-	-	55.5	-
	MaskPoint [56]	T+S	-	84.4	86.0	-	-	-
	FPS-Net [61]	R+F	-	-	-	-	57.1	-
	Densepoint [64]	T+S	-	84.2	86.4	-	-	-
	CrossPoint [66]	T+R+S+F+D+J	-	-	85.5	-	-	-
3D-MiniNet-KNN [70]	T+R+F+D	-	-	-	28.00	55.8	-	
2DPASS [72]	R+S+F	-	-	-	16.13	72.9	-	
Advanced	Mix3D [124]	Others	Rigid KPCConv [138]	-	-	-	63.6	66.6

4.2.3 Classification

For point cloud classification, ModelNet10 and ModelNet40 [85] are commonly used synthetic point cloud datasets, and ScanObjectNN[139] is a commonly used real-world point cloud dataset. The performance of relevant methods on these datasets is shown in Table 7.

Thanks to the powerful Transformer model, MaskPoint [56] achieves the best performance in ScanObjectNN when using a simple combination of translation and scaling. For classification tasks, mixup augmentation methods perform well, likely because generalization ability can be obtained by fitting the model in mixed samples. At present, mixup augmentation is probably the most popular type of advanced method for classification. Transformer-based baselines with mixup augmentation may achieve better performance in the future.

Both patch-based augmentation and auto optimization augmentation methods produced good overall results in ModelNet and ScanObjectNN datasets. In contrast to mixup methods, their application is not limited to classification. However, the research in these two types of augmentation methods is still very limited, and there is potential for development in the future.

Table 7. Comparative results of representative methods for the classification task on the ModelNet and ScanObjectNN benchmark. OA is used for evaluation metrics. The '%' after the value is omitted. '-' means that the result is not available. The values in italics come from replicated tests by others. 'T', 'R', 'S', 'F', 'D', 'J' represent Translation, Rotation, Scaling, Flipping, Drop, Jittering, respectively.

Method	Baseline	ModelNet		ScanObjectNN			
		ModelNet40(OA)	ModelNet10(OA)	OBJ_ONLY (OA)	PB_T50_RS (OA)		
Basic	IPC-Net [12]	D	-	93.7	-	86.7	-
	SPHNet [6]	R	-	87.1	-	-	-
	RI-GCN [9]	R	-	91	-	-	-
	PointWOLF [36]	Patch-based (T+R+S+D+J)	PointNet++ [38]	93.2	-	89.7	84.1
	PatchAugment [37]	Patch-based (T+R+S+D+J)	DGCNN [137] PointNet++ [38]	93.1 93	95.6 95.6	86.9 85.7	79.7 81
	AdaPC [74]	Auto optimization (T+R+S+J)	-	91.61	-	81.75	-
	PointAugment [73]	Auto optimization (T+R+S+J)	DGCNN [137]	93.4	96.7	83.1	76.8
	Pointnet++ [38]	T+R	-	91.9	-	<i>84.3</i>	<i>77.9</i>
	Shape Self-Correction [44]	T+R+S+D	RSCNN[46]	93.0	95.5	-	-
	RS-CNN [46]	T+S+D	-	93.6	-	-	-
	PointNet [48]	R+J	-	89.2	-	79.2	68.0
	MaskPoint [56]	T+S	-	-	-	89.7	84.6
Densepoint [64]	T+S	-	93.2	96.6	-	-	
CrossPoint [66]	T+R+S+F+D+J	DGCNN [137]	91.2	-	81.7	-	
Advanced	Luo et al. [88]	Mixup	-	87.6	94.2	-	-
	PC-GAN [87]	Mixup	-	<i>84.5</i>	<i>95.4</i>	-	-
	Achlioptas et al. [79]	Mixup	-	84.5	95.4	-	-
	Point MixSwap [86]	Mixup	DGCNN [137]	93.5	96	88.6	-
	PointMixup [80]	Mixup	DGCNN [137]	<i>93.1</i>	<i>95.1</i>	<i>87.6</i>	<i>80.6</i>
	RSMix [81]	Mixup	DGCNN [137]	93.5	95.9	-	-
	PointCutMix [82]	Mixup	PointNet++ [38]	93.4	96.3	88.47	82.8
	FMix [84]	Mixup	PointNet [48]	-	89.57	-	-
	MaxUp [102]	Adversarial deformation	-	92.4	-	-	-

4.2.4 Summary

At present, point cloud data augmentation for various tasks, especially advanced point cloud augmentation, is still in the stage of rapid development. For detection and segmentation, GT-sampling and other basic operations are often combined to augment point cloud data. However, there are very limited number of advanced methods that have been evaluated against the commonly used benchmark datasets for detection and segmentation. For classification, the commonly used

basic operations include translation, rotation, scaling, jittering and drop, while the most commonly used advanced method is mixup augmentation.

Although the advanced point cloud augmentation methods perform well in the benchmark datasets, they do not seem to shake the performance of a decent combination of easy-to-use and effective basic augmentation methods. As such, most augmentation strategies currently considered for point cloud processing tasks tend to use combinations of basic operations.

However, it should be noted that the reported performance is the result of combined contributions of augmentation methods and DL networks. Ideally, the same baseline network (e.g. PV-RCNN in Table 3 and DGCNN in Table 7) should be considered to allow for a fairer comparison of the performance of different augmentation methods. However, researchers usually tend to maximize the overall performance of a point cloud processing task, by choosing the best combination of augmentation and DL network. Therefore, performance testing under the same baseline network(s) is still limited, which may be worth further investigation. Based on the reported performance results, the best-performing combination usually involves the use of Transformer networks.

5 Conclusion

Point cloud data augmentation can effectively improve the performance of DL models for point cloud processing and analysis. This article provides the first comprehensive survey of various point cloud data augmentation methods, under the proposed taxonomy framework. In addition, this article summarizes and compares the augmentation methods used by the best-performing combination of augmentation and DL network in each representative study considered.

Currently, point cloud data augmentation methods, especially advanced methods, are under rapid development. Combined with an appropriate DL network, basic augmentation methods can be used to achieve better performance than advanced methods in point cloud processing tasks. For detection and segmentation tasks, the combination of GT-sampling and other basic operations is still the mainstream means of point cloud data augmentation. In classification tasks, translation, rotation, scaling, jittering and drop are the most widely used basic operations, and mixup augmentation is the mainstream advanced method.

Based on our survey, it seems that researchers have not specifically investigate up-sampling and generative models to perform point cloud data augmentation. With the rapid development of research on GAN and diffusion models, these models can be used for point cloud up-sampling and generation. Therefore, for future study, it is useful to evaluate these promising augmentation approaches on popular benchmark datasets that are specific to particular point cloud processing tasks, to determine their effectiveness as point cloud data augmentation techniques. In addition, existing research does not fully explore the integration of basic and advanced methods. Future research can target this integration for potential improvements in performance.

Currently, there are few dedicated studies to test the performance of point cloud data augmentation methods under the same baseline network for various point cloud processing tasks. Such tests will be useful for more accurately understanding the performance of different augmentation methods, and can be considered in future research. This may also need dedicated evaluation metrics tailored to evaluate the effectiveness of point cloud data augmentation techniques, and dedicated benchmark datasets. Since Transformer networks have achieved strong performance in segmentation and classification tasks even when using simple combination of basic operations, it is interesting to explore how more advanced augmentations perform under the state-of-the-art Transformers as the baseline networks.

Reference

1. Feng SY, Gangal V, Wei J, Chandar S, Vosoughi S, Mitamura T, et al. A survey of data augmentation approaches for NLP. arXiv preprint arXiv:210503075. 2021.
2. Shorten C, Khoshgoftaar TM. A survey on image data augmentation for deep learning. *Journal of big data*. 2019;6(1):1-48.
3. Choi J, Song Y, Kwak N, editors. Part-aware data augmentation for 3d object detection in point cloud. 2021 IEEE/RSJ International Conference on Intelligent Robots and Systems (IROS); 2021: IEEE.
4. Lai X, Liu J, Jiang L, Wang L, Zhao H, Liu S, et al., editors. Stratified transformer for 3d point cloud segmentation. *Proceedings of the IEEE/CVF Conference on Computer Vision and Pattern Recognition*; 2022.
5. Hamraz H, Jacobs NB, Contreras MA, Clark CH. Deep learning for conifer/deciduous classification of airborne LiDAR 3D point clouds representing individual trees. *ISPRS Journal of Photogrammetry and Remote Sensing*. 2019;158:219-30.
6. Poulenard A, Rakotosaona M-J, Ponty Y, Ovsjanikov M, editors. Effective rotation-invariant point cnn with spherical harmonics kernels. 2019 International Conference on 3D Vision (3DV); 2019: IEEE.
7. Liu X, Yan M, Bohg J, editors. Meteornet: Deep learning on dynamic 3d point cloud sequences. *Proceedings of the IEEE/CVF International Conference on Computer Vision*; 2019.
8. Zhang Y, Zhou Z, David P, Yue X, Xi Z, Gong B, et al., editors. Polarnet: An improved grid representation for online lidar point clouds semantic segmentation. *Proceedings of the IEEE/CVF Conference on Computer Vision and Pattern Recognition*; 2020.
9. Kim S, Park J, Han B. Rotation-invariant local-to-global representation learning for 3d point cloud. *Advances in Neural Information Processing Systems*. 2020;33:8174-85.
10. Griffiths D, Boehm J. Weighted point cloud augmentation for neural network training data class-imbalance. *The International Archives of the Photogrammetry, Remote Sensing and Spatial Information Sciences*. 2019;XLII-2/W13:981-7.
11. Zhang Z, Girdhar R, Joulin A, Misra I, editors. Self-supervised pretraining of 3d features on any point-cloud. *Proceedings of the IEEE/CVF International Conference on Computer Vision*; 2021.
12. He Y, Zhang Z, Wang Z, Luo Y, Su L, Li W, et al. IPC-Net: Incomplete point cloud classification network based on data augmentation and similarity measurement. *Journal of Visual Communication and Image Representation*. 2023;91:103769.
13. Ma W, Chen J, Du Q, Jia W, editors. PointDrop: Improving object detection from sparse point clouds via adversarial data augmentation. 2020 25th International Conference on Pattern Recognition (ICPR); 2021: IEEE.
14. Zhang Z, Xie S, Chen M, Zhu H. HandAugment: A simple data augmentation method for depth-based 3D hand pose estimation. arXiv preprint arXiv:200100702. 2020.
15. Li D, Shi G, Li J, Chen Y, Zhang S, Xiang S, et al. PlantNet: A dual-function point cloud segmentation network for multiple plant species. *ISPRS Journal of Photogrammetry and Remote Sensing*. 2022;184:243-63.
16. Yan Y, Mao Y, Li B. Second: Sparsely embedded convolutional detection. *Sensors*. 2018;18(10):3337.
17. Zhou Z, Zhang Y, Foroosh H, editors. Panoptic-polarnet: Proposal-free lidar point cloud panoptic segmentation. *Proceedings of the IEEE/CVF Conference on Computer Vision and Pattern Recognition*; 2021.
18. Lang AH, Vora S, Caesar H, Zhou L, Yang J, Beijbom O, editors. Pointpillars: Fast encoders for object detection from point clouds. *Proceedings of the IEEE/CVF conference on computer vision and pattern recognition*; 2019.

19. Shi S, Wang X, Li H, editors. Pointcnn: 3d object proposal generation and detection from point cloud. Proceedings of the IEEE/CVF conference on computer vision and pattern recognition; 2019.
20. Shi S, Guo C, Jiang L, Wang Z, Shi J, Wang X, et al., editors. Pv-rcnn: Point-voxel feature set abstraction for 3d object detection. Proceedings of the IEEE/CVF conference on computer vision and pattern recognition; 2020.
21. Wang T, Zhu X, Lin D, editors. Reconfigurable voxels: A new representation for lidar-based point clouds. Conference on Robot Learning; 2021: PMLR.
22. Yang Z, Sun Y, Liu S, Shen X, Jia J, editors. Std: Sparse-to-dense 3d object detector for point cloud. Proceedings of the IEEE/CVF international conference on computer vision; 2019.
23. He C, Zeng H, Huang J, Hua X-S, Zhang L, editors. Structure aware single-stage 3d object detection from point cloud. Proceedings of the IEEE/CVF conference on computer vision and pattern recognition; 2020.
24. Hu P, Ziglar J, Held D, Ramanan D, editors. What you see is what you get: Exploiting visibility for 3d object detection. Proceedings of the IEEE/CVF Conference on Computer Vision and Pattern Recognition; 2020.
25. Zhou Y, Sun P, Zhang Y, Anguelov D, Gao J, Ouyang T, et al., editors. End-to-end multi-view fusion for 3d object detection in lidar point clouds. Conference on Robot Learning; 2020: PMLR.
26. Chen Q, Sun L, Wang Z, Jia K, Yuille A, editors. Object as hotspots: An anchor-free 3d object detection approach via firing of hotspots. Computer Vision–ECCV 2020: 16th European Conference, Glasgow, UK, August 23–28, 2020, Proceedings, Part XXI 16; 2020: Springer.
27. Chen Y, Liu S, Shen X, Jia J, editors. Fast point r-cnn. Proceedings of the IEEE/CVF international conference on computer vision; 2019.
28. Hu X, Duan Z, Ma J. Context-Aware Data Augmentation for LIDAR 3D Object Detection. arXiv preprint arXiv:221110850. 2022.
29. Kong L, Liu Y, Chen R, Ma Y, Zhu X, Li Y, et al. Rethinking range view representation for lidar segmentation. arXiv preprint arXiv:230305367. 2023.
30. Zhu B, Jiang Z, Zhou X, Li Z, Yu G. Class-balanced grouping and sampling for point cloud 3d object detection. arXiv preprint arXiv:190809492. 2019.
31. Wang C, Ma C, Zhu M, Yang X, editors. Pointaugmenting: Cross-modal augmentation for 3d object detection. Proceedings of the IEEE/CVF Conference on Computer Vision and Pattern Recognition; 2021.
32. Hasecke F, Alsfasser M, Kummert A, editors. What can be seen is what you get: Structure aware point cloud augmentation. 2022 IEEE Intelligent Vehicles Symposium (IV); 2022: IEEE.
33. Xiao W, Li X, Liu C, Gao J, Luo J, Peng Y, et al. 3D-VDNet: Exploiting the vertical distribution characteristics of point clouds for 3D object detection and augmentation. Image and Vision Computing. 2022;127:104557.
34. Xiao A, Huang J, Guan D, Cui K, Lu S, Shao L. Polarmix: A general data augmentation technique for lidar point clouds. Advances in Neural Information Processing Systems. 2022;35:11035-48.
35. Zheng W, Tang W, Jiang L, Fu C-W, editors. SE-SSD: Self-ensembling single-stage object detector from point cloud. Proceedings of the IEEE/CVF Conference on Computer Vision and Pattern Recognition; 2021.
36. Kim S, Lee S, Hwang D, Lee J, Hwang SJ, Kim HJ, editors. Point cloud augmentation with weighted local transformations. Proceedings of the IEEE/CVF International Conference on Computer Vision; 2021.
37. Sheshappanavar SV, Singh VV, Kambhamettu C, editors. Patchaugment: Local neighborhood augmentation in point cloud classification. Proceedings of the IEEE/CVF International Conference on Computer Vision; 2021.

38. Qi CR, Yi L, Su H, Guibas LJ. Pointnet++: Deep hierarchical feature learning on point sets in a metric space. *Advances in neural information processing systems*. 2017;30.
39. Hahner M, Dai D, Liniger A, Van Gool L. Quantifying data augmentation for lidar based 3d object detection. *arXiv preprint arXiv:200401643*. 2020.
40. Zhou Y, Tuzel O, editors. Voxelnet: End-to-end learning for point cloud based 3d object detection. *Proceedings of the IEEE conference on computer vision and pattern recognition*; 2018.
41. Ye M, Cao T, Chen Q, editors. Tpcn: Temporal point cloud networks for motion forecasting. *Proceedings of the IEEE/CVF Conference on Computer Vision and Pattern Recognition*; 2021.
42. Chaton T, Chaulet N, Horache S, Landrieu L, editors. Torch-Points3D: A modular multi-task framework for reproducible deep learning on 3D point clouds. *2020 International Conference on 3D Vision (3DV)*; 2020: IEEE.
43. Ngiam J, Caine B, Han W, Yang B, Chai Y, Sun P, et al. Starnet: Targeted computation for object detection in point clouds. *arXiv preprint arXiv:190811069*. 2019.
44. Chen Y, Liu J, Ni B, Wang H, Yang J, Liu N, et al., editors. Shape self-correction for unsupervised point cloud understanding. *Proceedings of the IEEE/CVF International Conference on Computer Vision*; 2021.
45. Tchapmi L, Choy C, Armeni I, Gwak J, Savarese S, editors. Segcloud: Semantic segmentation of 3d point clouds. *2017 international conference on 3D vision (3DV)*; 2017: IEEE.
46. Liu Y, Fan B, Xiang S, Pan C, editors. Relation-shape convolutional neural network for point cloud analysis. *Proceedings of the IEEE/CVF conference on computer vision and pattern recognition*; 2019.
47. Wang G, Wu X, Liu Z, Wang H, editors. Pwclo-net: Deep lidar odometry in 3d point clouds using hierarchical embedding mask optimization. *Proceedings of the IEEE/CVF conference on computer vision and pattern recognition*; 2021.
48. Qi CR, Su H, Mo K, Guibas LJ, editors. Pointnet: Deep learning on point sets for 3d classification and segmentation. *Proceedings of the IEEE conference on computer vision and pattern recognition*; 2017.
49. Shi W, Rajkumar R, editors. Point-gnn: Graph neural network for 3d object detection in a point cloud. *Proceedings of the IEEE/CVF conference on computer vision and pattern recognition*; 2020.
50. Yang B, Luo W, Urtasun R, editors. Pixor: Real-time 3d object detection from point clouds. *Proceedings of the IEEE conference on Computer Vision and Pattern Recognition*; 2018.
51. Guo M-H, Cai J-X, Liu Z-N, Mu T-J, Martin RR, Hu S-M. Pct: Point cloud transformer. *Computational Visual Media*. 2021;7:187-99.
52. Qi CR, Zhou Y, Najibi M, Sun P, Vo K, Deng B, et al., editors. Offboard 3d object detection from point cloud sequences. *Proceedings of the IEEE/CVF Conference on Computer Vision and Pattern Recognition*; 2021.
53. Liang M, Yang B, Chen Y, Hu R, Urtasun R, editors. Multi-task multi-sensor fusion for 3d object detection. *Proceedings of the IEEE/CVF Conference on Computer Vision and Pattern Recognition*; 2019.
54. Alnaggar YA, Afifi M, Amer K, ElHelw M, editors. Multi projection fusion for real-time semantic segmentation of 3d lidar point clouds. *Proceedings of the IEEE/CVF winter conference on applications of computer vision*; 2021.
55. Komorowski J, editor. Minkloc3d: Point cloud based large-scale place recognition. *Proceedings of the IEEE/CVF Winter Conference on Applications of Computer Vision*; 2021.
56. Liu H, Cai M, Lee YJ, editors. Masked discrimination for self-supervised learning on point clouds. *European Conference on Computer Vision*; 2022: Springer.
57. Nguyen DT, Quach M, Valenzise G, Duhamel P. Lossless coding of point cloud geometry using a deep generative model. *IEEE Transactions on Circuits and Systems for Video Technology*. 2021;31(12):4617-29.

58. Kong L, Ren J, Pan L, Liu Z, editors. Lasermix for semi-supervised lidar semantic segmentation. Proceedings of the IEEE/CVF Conference on Computer Vision and Pattern Recognition; 2023.
59. Zheng Y, Li Y, Yang S, Lu H. Global-PBNet: A novel point cloud registration for autonomous driving. IEEE Transactions on Intelligent Transportation Systems. 2022;23(11):22312-9.
60. Wang Z, Jia K, editors. Frustum convnet: Sliding frustums to aggregate local point-wise features for amodal 3d object detection. 2019 IEEE/RSJ International Conference on Intelligent Robots and Systems (IROS); 2019: IEEE.
61. Xiao A, Yang X, Lu S, Guan D, Huang J. FPS-Net: A convolutional fusion network for large-scale LiDAR point cloud segmentation. ISPRS Journal of Photogrammetry and Remote Sensing. 2021;176:237-49.
62. Zhao N, Chua T-S, Lee GH, editors. Few-shot 3d point cloud semantic segmentation. Proceedings of the IEEE/CVF Conference on Computer Vision and Pattern Recognition; 2021.
63. Li J, Bi Y, Lee GH, editors. Discrete rotation equivariance for point cloud recognition. 2019 International conference on robotics and automation (ICRA); 2019: IEEE.
64. Liu Y, Fan B, Meng G, Lu J, Xiang S, Pan C, editors. Densepoint: Learning densely contextual representation for efficient point cloud processing. Proceedings of the IEEE/CVF international conference on computer vision; 2019.
65. Liang M, Yang B, Wang S, Urtasun R, editors. Deep continuous fusion for multi-sensor 3d object detection. Proceedings of the European conference on computer vision (ECCV); 2018.
66. Afham M, Dissanayake I, Dissanayake D, Dharmasiri A, Thilakarathna K, Rodrigo R, editors. Crosspoint: Self-supervised cross-modal contrastive learning for 3d point cloud understanding. Proceedings of the IEEE/CVF Conference on Computer Vision and Pattern Recognition; 2022.
67. Hu Y, Ding Z, Ge R, Shao W, Huang L, Li K, et al., editors. Afdetv2: Rethinking the necessity of the second stage for object detection from point clouds. Proceedings of the AAAI Conference on Artificial Intelligence; 2022.
68. Choy C, Gwak J, Savarese S, editors. 4d spatio-temporal convnets: Minkowski convolutional neural networks. Proceedings of the IEEE/CVF conference on computer vision and pattern recognition; 2019.
69. Wang H, Cong Y, Litany O, Gao Y, Guibas LJ, editors. 3dioumatch: Leveraging iou prediction for semi-supervised 3d object detection. Proceedings of the IEEE/CVF Conference on Computer Vision and Pattern Recognition; 2021.
70. Alonso I, Riazuelo L, Montesano L, Murillo AC. 3d-mininet: Learning a 2d representation from point clouds for fast and efficient 3d lidar semantic segmentation. IEEE Robotics and Automation Letters. 2020;5(4):5432-9.
71. Horache S, Deschaud J-E, Goulette F, editors. 3D point cloud registration with multi-scale architecture and unsupervised transfer learning. 2021 international conference on 3D vision (3DV); 2021: IEEE.
72. Yan X, Gao J, Zheng C, Zheng C, Zhang R, Cui S, et al., editors. 2dpass: 2d priors assisted semantic segmentation on lidar point clouds. European Conference on Computer Vision; 2022: Springer.
73. Li R, Li X, Heng P-A, Fu C-W, editors. Pointaugment: an auto-augmentation framework for point cloud classification. Proceedings of the IEEE/CVF conference on computer vision and pattern recognition; 2020.
74. Zhang W, Xu X, Liu F, Zhang L, Foo C-S. On automatic data augmentation for 3D point cloud classification. arXiv preprint arXiv:211206029. 2021.
75. Cheng S, Leng Z, Cubuk ED, Zoph B, Bai C, Ngiam J, et al., editors. Improving 3d object detection through progressive population based augmentation. Computer Vision–ECCV 2020: 16th

European Conference, Glasgow, UK, August 23–28, 2020, Proceedings, Part XXI 16; 2020: Springer.

76. Leng Z, Li G, Liu C, Cubuk ED, Sun P, He T, et al., editors. Lidar Augment: Searching for Scalable 3D LiDAR Data Augmentations. 2023 IEEE International Conference on Robotics and Automation (ICRA); 2023: IEEE.
77. Zhang H, Cisse M, Dauphin YN, Lopez-Paz D. Mixup: Beyond empirical risk minimization. arXiv preprint arXiv:171009412. 2017.
78. Groueix T, Fisher M, Vladimir, Bryan, Aubry M. AtlasNet: A Papier-M^{ach} Approach to Learning 3D Surface Generation. arXiv pre-print server. 2018.
79. Achlioptas P, Diamanti O, Mitliagkas I, Guibas L, editors. Learning representations and generative models for 3d point clouds. International conference on machine learning; 2018: PMLR.
80. Chen Y, Hu VT, Gavves E, Mensink T, Mettes P, Yang P, et al., editors. Pointmixup: Augmentation for point clouds. Computer Vision–ECCV 2020: 16th European Conference, Glasgow, UK, August 23–28, 2020, Proceedings, Part III 16; 2020: Springer.
81. Lee D, Lee J, Lee J, Lee H, Lee M, Woo S, et al., editors. Regularization strategy for point cloud via rigidly mixed sample. Proceedings of the IEEE/CVF Conference on Computer Vision and Pattern Recognition; 2021.
82. Zhang J, Chen L, Ouyang B, Liu B, Zhu J, Chen Y, et al. Pointcutmix: Regularization strategy for point cloud classification. *Neurocomputing*. 2022;505:58-67.
83. Liu M, Sheng L, Yang S, Shao J, Hu S-M, editors. Morphing and sampling network for dense point cloud completion. Proceedings of the AAAI conference on artificial intelligence; 2020.
84. Harris E, Marcu A, Painter M, Niranjana M, Prügel-Bennett A, Hare J. Fmix: Enhancing mixed sample data augmentation. arXiv preprint arXiv:200212047. 2020.
85. Wu Z, Song S, Khosla A, Yu F, Zhang L, Tang X, et al., editors. 3d shapenets: A deep representation for volumetric shapes. Proceedings of the IEEE conference on computer vision and pattern recognition; 2015.
86. Umam A, Yang C-K, Chuang Y-Y, Chuang J-H, Lin Y-Y, editors. Point mixswap: Attentional point cloud mixing via swapping matched structural divisions. European Conference on Computer Vision; 2022: Springer.
87. Li C-L, Zaheer M, Zhang Y, Póczos B, Salakhutdinov R. Point cloud gan. arXiv preprint arXiv:181005795. 2018.
88. Luo S, Hu W, editors. Diffusion probabilistic models for 3d point cloud generation. Proceedings of the IEEE/CVF Conference on Computer Vision and Pattern Recognition; 2021.
89. Chen Z, Luo Y, Huang Z, Wang Z, Baktashmotlagh M. Revisiting Domain-Adaptive 3D Object Detection by Reliable, Diverse and Class-balanced Pseudo-Labeling. arXiv preprint arXiv:230707944. 2023.
90. Goodin C, Carruth D, Doude M, Hudson C. Predicting the Influence of Rain on LIDAR in ADAS. *Electronics*. 2019;8(1):89.
91. Bijelic M, Gruber T, Mannan F, Kraus F, Ritter W, Dietmayer K, et al., editors. Seeing through fog without seeing fog: Deep multimodal sensor fusion in unseen adverse weather. Proceedings of the IEEE/CVF Conference on Computer Vision and Pattern Recognition; 2020.
92. Hahner M, Sakaridis C, Dai D, Van Gool L, editors. Fog simulation on real LiDAR point clouds for 3D object detection in adverse weather. Proceedings of the IEEE/CVF International Conference on Computer Vision; 2021.
93. Hahner M, Sakaridis C, Bijelic M, Heide F, Yu F, Dai D, et al., editors. Lidar snowfall simulation for robust 3d object detection. Proceedings of the IEEE/CVF Conference on Computer Vision and Pattern Recognition; 2022.
94. Kilic V, Hegde D, Sindagi V, Cooper AB, Foster MA, Patel VM. Lidar light scattering augmentation (lisa): Physics-based simulation of adverse weather conditions for 3d object detection. arXiv preprint arXiv:210707004. 2021.

95. Hu JS, Waslander SL, editors. Pattern-aware data augmentation for lidar 3d object detection. 2021 IEEE International Intelligent Transportation Systems Conference (ITSC); 2021: IEEE.
96. Matuszka T, Kozma D, editors. A novel neural network training method for autonomous driving using semi-pseudo-labels and 3d data augmentations. Asian Conference on Intelligent Information and Database Systems; 2022: Springer.
97. Deng L, Yang M, Li H, Li T, Hu B, Wang C. Restricted deformable convolution-based road scene semantic segmentation using surround view cameras. *IEEE Transactions on Intelligent Transportation Systems*. 2019;21(10):4350-62.
98. Sallab AE, Sobh I, Zahran M, Essam N. LiDAR Sensor modeling and Data augmentation with GANs for Autonomous driving. arXiv preprint arXiv:190507290. 2019.
99. Zhu J-Y, Park T, Isola P, Efros AA, editors. Unpaired image-to-image translation using cycle-consistent adversarial networks. *Proceedings of the IEEE international conference on computer vision*; 2017.
100. Ryu K, Hwang S, Park J, editors. Instant Domain Augmentation for LiDAR Semantic Segmentation. *Proceedings of the IEEE/CVF Conference on Computer Vision and Pattern Recognition*; 2023.
101. Lehner A, Gasperini S, Marcos-Ramiro A, Schmidt M, Mahani M-AN, Navab N, et al., editors. 3D-VField: Adversarial augmentation of point clouds for domain generalization in 3D object detection. *Proceedings of the IEEE/CVF Conference on Computer Vision and Pattern Recognition*; 2022.
102. Gong C, Ren T, Ye M, Liu Q, editors. Maxup: Lightweight adversarial training with data augmentation improves neural network training. *Proceedings of the IEEE/CVF Conference on computer vision and pattern recognition*; 2021.
103. Tu J, Ren M, Manivasagam S, Liang M, Yang B, Du R, et al., editors. Physically realizable adversarial examples for lidar object detection. *Proceedings of the IEEE/CVF Conference on Computer Vision and Pattern Recognition*; 2020.
104. Wu M, Huang H, Fang Y, editors. 3d point cloud completion with geometric-aware adversarial augmentation. *2022 26th International Conference on Pattern Recognition (ICPR)*; 2022: IEEE.
105. Liu G, Liu J, Zhang Q, Fang C, Zhang X, editors. TauPad: test data augmentation of point clouds by adversarial mutation. *Proceedings of the ACM/IEEE 44th International Conference on Software Engineering: Companion Proceedings*; 2022.
106. Xiang C, Qi CR, Li B, editors. Generating 3d adversarial point clouds. *Proceedings of the IEEE/CVF Conference on Computer Vision and Pattern Recognition*; 2019.
107. Hamdi A, Rojas S, Thabet A, Ghanem B, editors. Advpc: Transferable adversarial perturbations on 3d point clouds. *Computer Vision—ECCV 2020: 16th European Conference, Glasgow, UK, August 23–28, 2020, Proceedings, Part XII 16*; 2020: Springer.
108. Zhao Y, Wu Y, Chen C, Lim A, editors. On isometry robustness of deep 3d point cloud models under adversarial attacks. *Proceedings of the IEEE/CVF Conference on Computer Vision and Pattern Recognition*; 2020.
109. Wang W, Huang Q, You S, Yang C, Neumann U, editors. Shape inpainting using 3d generative adversarial network and recurrent convolutional networks. *Proceedings of the IEEE international conference on computer vision*; 2017.
110. Valsesia D, Fracastoro G, Magli E, editors. Learning localized generative models for 3d point clouds via graph convolution. *International conference on learning representations*; 2018.
111. Li R, Li X, Fu C-W, Cohen-Or D, Heng P-A, editors. Pu-gan: a point cloud upsampling adversarial network. *Proceedings of the IEEE/CVF international conference on computer vision*; 2019.
112. Chang AX, Funkhouser T, Guibas L, Hanrahan P, Huang Q, Li Z, et al. Shapenet: An information-rich 3d model repository. arXiv preprint arXiv:151203012. 2015.

113. Yu Y, Huang Z, Li F, Zhang H, Le X. Point Encoder GAN: A deep learning model for 3D point cloud inpainting. *Neurocomputing*. 2020;384:192-9.
114. Yan X, Gao J, Li J, Zhang R, Li Z, Huang R, et al., editors. Sparse single sweep lidar point cloud segmentation via learning contextual shape priors from scene completion. *Proceedings of the AAAI Conference on Artificial Intelligence*; 2021.
115. Lyu Z, Kong Z, Xu X, Pan L, Lin D. A conditional point diffusion-refinement paradigm for 3d point cloud completion. *arXiv preprint arXiv:211203530*. 2021.
116. Shu DW, Park SW, Kwon J, editors. 3d point cloud generative adversarial network based on tree structured graph convolutions. *Proceedings of the IEEE/CVF international conference on computer vision*; 2019.
117. Yang B, Wen H, Wang S, Clark R, Markham A, Trigoni N, editors. 3d object reconstruction from a single depth view with adversarial learning. *Proceedings of the IEEE International Conference on Computer Vision Workshops*; 2017.
118. Yang G, Huang X, Hao Z, Liu M-Y, Belongie S, Hariharan B, editors. Pointflow: 3d point cloud generation with continuous normalizing flows. *Proceedings of the IEEE/CVF international conference on computer vision*; 2019.
119. Cai R, Yang G, Averbuch-Elor H, Hao Z, Belongie S, Snavely N, et al., editors. Learning gradient fields for shape generation. *Computer Vision—ECCV 2020: 16th European Conference, Glasgow, UK, August 23–28, 2020, Proceedings, Part III 16*; 2020: Springer.
120. Vora S, Lang AH, Helou B, Beijbom O, editors. Pointpainting: Sequential fusion for 3d object detection. *Proceedings of the IEEE/CVF conference on computer vision and pattern recognition*; 2020.
121. Yin T, Zhou X, Krähenbühl P. Multimodal virtual point 3d detection. *Advances in Neural Information Processing Systems*. 2021;34:16494-507.
122. Fang J, Zuo X, Zhou D, Jin S, Wang S, Zhang L, editors. Lidar-aug: A general rendering-based augmentation framework for 3d object detection. *Proceedings of the IEEE/CVF Conference on Computer Vision and Pattern Recognition*; 2021.
123. Yang X, del Rey Castillo E, Zou Y, Wotherspoon L. Semantic segmentation of bridge point clouds with a synthetic data augmentation strategy and graph-structured deep metric learning. *Automation in Construction*. 2023;150:104838.
124. Nekrasov A, Schult J, Litany O, Leibe B, Engelmann F, editors. Mix3d: Out-of-context data augmentation for 3d scenes. *2021 International Conference on 3D Vision (3DV)*; 2021: IEEE.
125. Liu C, Gao C, Liu F, Li P, Meng D, Gao X, editors. Hierarchical Supervision and Shuffle Data Augmentation for 3D Semi-Supervised Object Detection. *Proceedings of the IEEE/CVF Conference on Computer Vision and Pattern Recognition*; 2023.
126. Leng Z, Cheng S, Caine B, Wang W, Zhang X, Shlens J, et al., editors. Pseudoaugment: Learning to use unlabeled data for data augmentation in point clouds. *European conference on computer vision*; 2022: Springer.
127. Geiger A, Lenz P, Urtasun R, editors. Are we ready for autonomous driving? the kitti vision benchmark suite. *2012 IEEE conference on computer vision and pattern recognition*; 2012: IEEE.
128. Caesar H, Bankiti V, Lang AH, Vora S, Liong VE, Xu Q, et al., editors. nuscenes: A multimodal dataset for autonomous driving. *Proceedings of the IEEE/CVF conference on computer vision and pattern recognition*; 2020.
129. Sun P, Kretschmar H, Dotiwalla X, Chouard A, Patnaik V, Tsui P, et al., editors. Scalability in perception for autonomous driving: Waymo open dataset. *Proceedings of the IEEE/CVF conference on computer vision and pattern recognition*; 2020.
130. Shi S, Wang Z, Shi J, Wang X, Li H. From points to parts: 3d object detection from point cloud with part-aware and part-aggregation network. *IEEE transactions on pattern analysis and machine intelligence*. 2020;43(8):2647-64.

131. Behley J, Garbade M, Milioto A, Quenzel J, Behnke S, Stachniss C, et al., editors. Semantickitti: A dataset for semantic scene understanding of lidar sequences. Proceedings of the IEEE/CVF international conference on computer vision; 2019.
132. Vaswani A, Shazeer N, Parmar N, Uszkoreit J, Jones L, Gomez AN, et al. Attention is all you need. Advances in neural information processing systems. 2017;30.
133. Duan K, Bai S, Xie L, Qi H, Huang Q, Tian Q, editors. Centernet: Keypoint triplets for object detection. Proceedings of the IEEE/CVF international conference on computer vision; 2019.
134. Sun P, Tan M, Wang W, Liu C, Xia F, Leng Z, et al., editors. Swformer: Sparse window transformer for 3d object detection in point clouds. European Conference on Computer Vision; 2022: Springer.
135. Tang H, Liu Z, Zhao S, Lin Y, Lin J, Wang H, et al., editors. Searching efficient 3d architectures with sparse point-voxel convolution. European conference on computer vision; 2020: Springer.
136. Zhu X, Zhou H, Wang T, Hong F, Ma Y, Li W, et al., editors. Cylindrical and asymmetrical 3d convolution networks for lidar segmentation. Proceedings of the IEEE/CVF conference on computer vision and pattern recognition; 2021.
137. Wang Y, Sun Y, Liu Z, Sarma SE, Bronstein MM, Solomon JM. Dynamic graph cnn for learning on point clouds. ACM Transactions on Graphics (tog). 2019;38(5):1-12.
138. Thomas H, Qi CR, Deschaud J-E, Marcotegui B, Goulette F, Guibas LJ, editors. Kpconv: Flexible and deformable convolution for point clouds. Proceedings of the IEEE/CVF international conference on computer vision; 2019.
139. Uy MA, Pham Q-H, Hua B-S, Nguyen T, Yeung S-K, editors. Revisiting point cloud classification: A new benchmark dataset and classification model on real-world data. Proceedings of the IEEE/CVF international conference on computer vision; 2019.